T2R2 東京工業大学リサーチリポジトリ
Tokyo Tech Research Repository

論文 / 著書情報
Article / Book Information

論題(和文)	WIND FORCE ESTIMATION ON A BASE-ISOLATED BUILDING USING MODAL ANALYSIS
Title(English)	WIND FORCE ESTIMATION ON A BASE-ISOLATED BUILDING USING MODAL ANALYSIS
著者(和文)	SORIANO Razelle Dennise A., 佐藤大樹, Alex Shegay
Authors(English)	Razelle Dennise Agoba Soriano, Daiki Sato, Aleksey Vadimovich Shegay
出典 / Citation	日本建築学会関東支部研究報告集, Ⅰ, , pp. 277-280
Citation(English)	, Ⅰ, , pp. 277-280
発行日 / Pub. date	2022, 3

Powered by T2R2 (Tokyo Institute Research Repository)

2021年度日本建築学会
関東支部研究報告集 I
2022年3月

WIND FORCE ESTIMATION ON A BASE-ISOLATED BUILDING USING MODAL ANALYSIS

構造ー振動　　正会員 ○ SORIANO Razelle Dennise A.*1　　同　佐藤 大樹*2
同　SHEGAY, Alex*3

Wind force estimation, Modal analysis, FDD Method
Base-isolation, Response identification, System identification

1. INTRODUCTION

1.1. Background

Advancements in structural engineering and technologies has increased the versatility of base-isolation devices resulting in wider adoption in high-rise buildings [1]. These buildings are tall and have been becoming overall lighter, making them more susceptible to large dynamic excitation from wind forces. Thus, wind load analysis is an important consideration in the design process. Analyzing base-isolated structures subjected to strong wind forces requires an accurate estimate of the time-histories of the input wind loads. One way to do this is by utilizing the recorded response (e.g., accelerations) from monitoring systems installed on structures [2]. In this case, structural dynamic parameters such as the mode shapes, natural frequency and damping ratio must also be determined before the wind forces can be estimated.

A system identification method called Frequency Domain Decomposition (FDD) [3] is employed in this paper to estimate the dynamic parameters of a building model. Then, using the estimated parameters, output-only modal analysis is used to back-calculate the wind force input into the system. It should be noted that the classical formulations of the FDD method do not exactly fit the characteristics of the wind excitation and the model; that is, stationary Gaussian white noise input and lightly damped structures [3]. The typically high damping of the structure's isolation layer [4] increases the equivalent damping of the whole system, which makes it difficult to accurately estimate the system's dynamic parameters. However, since the method has notable advantages such as simple implementation, directivity, and familiarity, its limitations are investigated in this paper.

1.2 Objective

This paper aims to determine the input wind force on a model of a tall base-isolated building behaving elastically using modal analysis and estimate its modal parameters by the FDD method. The effect of isolation layer damping on the accuracy of the estimated wind forces is also investigated.

2. THEORETICAL BACKGROUND

2.1. Frequency Domain Decomposition (FDD)

The FDD method is a procedure used to estimate the modal parameters (mode shapes, natural frequency and damping ratio) using the system response without knowing the input force of the model [5]. The FDD procedure employed in this paper is based on Brincker et al. [3] and will not be fully discussed except for the parts that have been modified.

2.2. Equivalent Damping Calculation

The FDD damping ratio results need to be compared with the actual damping of the system. The actual damping of the system will be calculated as the equivalent damping ratio, using the approximation method by Biggs [6]. The equivalent first-mode damping ratio of the entire base-isolated model, ${}_1\zeta_{eq}$, is given by the following.

$$ {}_1\zeta_{eq} = \frac{\sum_{i=0}^{N} \zeta_i W_i}{\sum_{i=0}^{N} W_i} \quad \text{where} \quad \zeta_i = \frac{1}{4\pi}\frac{\Delta W_i}{W_i} \qquad \text{(1a-b)} $$

$$ W_i = \begin{cases} \frac{1}{2} k_i \delta_i^2 & (i = 1 \sim 10) \\ \frac{1}{2} k_0 \delta_0^2 & (i = 0) \end{cases} \qquad \text{(1c)} $$

$$ \Delta W_i = \begin{cases} \pi c_i \omega_u \delta_i^2 & (i = 1 \sim 10) \\ \pi c_0 \omega_0 \delta_0^2 & (i = 0) \end{cases} \qquad \text{(1d)} $$

where W_i and ΔW_i are the elastic strain energy, absorbed energy in the first cycle of the i th layer, ζ_i is the damping constant of the superstructure, δ_i is the inter-story drift at the i th layer $= u_i - u_{i-1}$ where mode shape ${}_s\phi_i$ is used for u instead of displacement, ω_u, k_i, ω_0, and k_0 are the first natural frequency and stiffness of the upper structure and the isolation layer, respectively.

2.3. Wind Force Estimation by Modal Analysis

The mass matrix of the model is calculated from the given structural properties using the following matrix equation

$$[M]=\begin{bmatrix} m_1 & 0 & \cdots & 0 \\ 0 & m_2 & \cdots & 0 \\ \vdots & \vdots & \ddots & \vdots \\ 0 & 0 & \cdots & m_N \end{bmatrix} \tag{2}$$

The 1st mode shape (${}_1\phi_i$) and the natural circular frequencies (${}_1\omega$ and ${}_2\omega$) and damping ratios (${}_1\zeta$ and ${}_2\zeta$) of the first and second modes of the system obtained from FDD analysis are used to estimate the wind forces. The system stiffness $[K]$ and damping $[C]$ matrices are calculated by

$$k_i = \frac{{}_1\omega^2 \cdot m_i \cdot {}_1\phi_i + k_{i+1}({}_1\phi_{i+1} - {}_1\phi_i)}{{}_1\phi_i - {}_1\phi_{i-1}} \qquad (i = 1 \sim N), \tag{3a}$$

$$[K]=\begin{bmatrix} k_1+k_2 & -k_2 & \cdots & 0 \\ -k_2 & k_2+k_3 & \cdots & 0 \\ \vdots & \vdots & \ddots & \vdots \\ 0 & 0 & \cdots & k_N \end{bmatrix} \tag{3b}$$

$$\begin{bmatrix} {}_1\zeta \\ {}_2\zeta \end{bmatrix} = \frac{1}{2}\begin{bmatrix} 1/{}_1\omega & {}_1\omega \\ 1/{}_2\omega & {}_2\omega \end{bmatrix}\begin{bmatrix} a_m \\ a_k \end{bmatrix} \tag{4a}$$

$$[C]=a_m[M]+a_k[K] \tag{4b}$$

where m_i is the mass of ith layer, $N = 11$ which is the number of degrees-of-freedom (DOF), and a_m and a_k are the Rayleigh damping coefficients. After obtaining the structural matrices, the mode shape matrix $[\Phi]$ can be calculated using eigenvalue analysis and the generalized matrices and modal responses can be calculated using Eqs. (5) and (6), respectively. Substituting these values to Eq. (7) calculates the generalized wind forces $\{{}_sP(t)\}$. The actual wind forces $\{P(t)\}$ can then be obtained by Eq. (8).

$$\begin{aligned} [{}_sM] &= [\Phi]^T[M][\Phi] \\ [{}_sC] &= [\Phi]^T[C][\Phi] \\ [{}_sK] &= [\Phi]^T[K][\Phi] \end{aligned} \tag{5a-c}$$

$$\{\ddot{x}(t)\} = [\Phi]\{\ddot{q}(t)\},\ \{\dot{x}(t)\} = [\Phi]\{\dot{q}(t)\} \text{ and } \{x(t)\} = [\Phi]\{q(t)\} \tag{6a-c}$$

$$[{}_sM]\{\ddot{q}(t)\} + [{}_sC]\{\dot{q}(t)\} + [{}_sK]\{q(t)\} = \{{}_sP(t)\} \tag{7}$$

$$\{P(t)\} = [\Phi]^{T^{-1}}\{{}_sP(t)\} \tag{8}$$

The accuracy of the calculated wind force is confirmed by calculating its correlation with the original wind force applied to the model. The correlation equation is given by Eq. (9) where $\hat{y}$ is the original wind force value and $\bar{y}$ is the mean of the estimated wind force value y. The conceptual framework of the analysis is shown in Figure 1.

$$Correlation = \left(1 - \frac{\sqrt{\sum_{k=1}^{N}(\hat{y}(k) - y(k))^2}}{\sqrt{\sum_{k=1}^{N}(y(k) - \bar{y})^2}}\right) \tag{9}$$

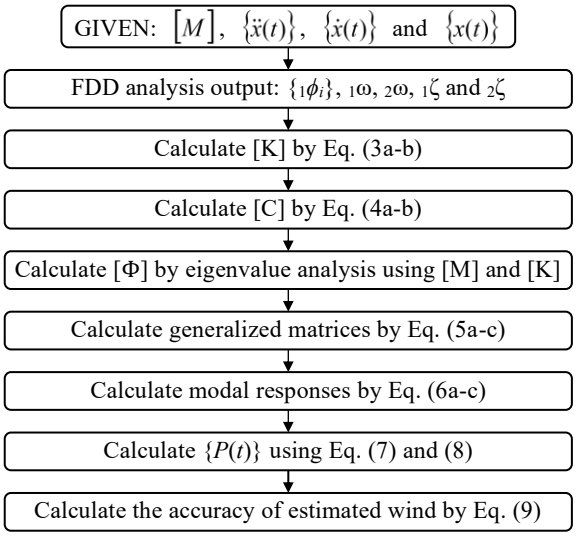

Figure 1. Analysis flowchart

3. OVERVIEW OF THE MODEL

3.1. Model Properties

Figure 2 shows the simplified 11-DOF lumped mass model of the building to be analyzed. The properties of the modeled building are also shown in this figure.

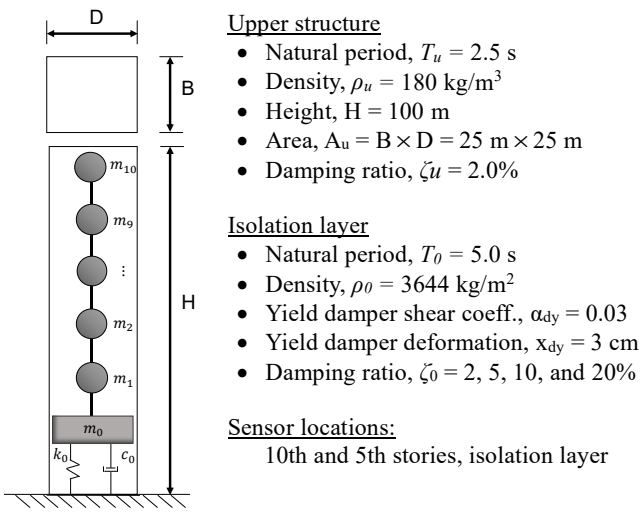

Figure 2. Analytical model properties

The isolation layer is assumed to behave elastically and its characteristics are determined from the following equations

$$Q_{dy} = \alpha_{dy}(W_u + W_0) \tag{10}$$

$$k_d = \frac{\alpha_{dy}(W_u + W_0)}{x_{dy}} \quad \text{and} \quad k_0 = \frac{4\pi^2(m_u + m_0)}{T_0^2} \qquad \text{(11a-b)}$$

$$k_{01} = k_d + k_0 \qquad \text{(12)}$$

where Q_{dy} is the yield strength of the isolation layer damper, k_d is the initial stiffness of the damper, k_0 is the stiffness of the isolator, W_u, m_u W_0, and m_0 are the total weight and mass of the upper structure and the base isolation, respectively, k_{01} is the primary stiffness of the isolation layer. The damping coefficient of the isolation layer and the upper structure, c_0 and c_i are calculated using the Eq. 13a-b. Varying damping ratios of the isolator are used as shown in Table 1. Wind data from a typhoon simulation in the across-wind direction of the building is applied to the model by multi degree-of-freedom analysis in order to obtain the responses (acceleration, velocity and displacement).

$$c_0 = \frac{2\zeta_0 k_{01}}{\omega_0} \quad \text{and} \quad c_i = \frac{2\zeta_u k_i}{\omega_u} \qquad \text{(13a-b)}$$

Table 1. Damping models

MODEL	Damping ratio (%)	
	Isolation layer	Upper structure
MH-02	2	2
MH-05	5	2
MH-10	10	2
MH-20	20	2

4. RESULTS OF ANALYSIS

4.1. Wind Force Estimation (All variables are known)

In order to check the accuracy of the method, the analysis is carried out assuming that all responses and structural parameters are known. The results of the correlation of the estimated wind forces for the upper floors (6th to 10th) are shown in Figure 3. An accurate estimate of the wind forces can be obtained when all modes are included in the modal superposition even for a high damping model (MH-20).

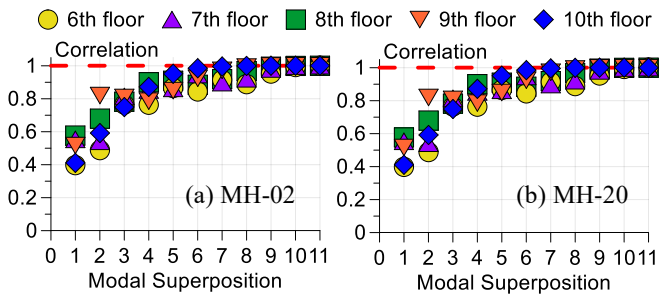

Figure 3. Estimated wind force correlation

4.2. FDD Mode Shape Estimation

In the FDD method, the first step is to calculate the power spectral density (PSD) of the response signal, in this case, the acceleration response. The obtained PSD is then decomposed in the frequency domain using the Singular Value Decomposition technique. The 1st singular values (SV) are considered sufficient to estimate the modal parameters of the models and an ensemble of 40 acceleration response time-history data were averaged to reduce the noise obtained in the SV. Figure 4 shows the SV plots of the different models. The peaks of models MH-02, MH-05 and MH-10 have the same frequency peaks. However, for the model with the highest damping ratio (MH-20), the 2nd peak is shifted to the right of the other three models. It is evident here that the FDD method has some limitations when used with a model that has a high damping ratio value. The s th peak of the 1st SV is then used to determine the mode shape of the s th mode of vibration. The accuracy of the estimated mode shapes is compared to the normalized maximum displacement response of the model in Figure 5a. It is observed here that as the damping ratio of the isolation layer increases, the accuracy of the estimated mode shape decreases.

4.3. FDD Natural frequency and Damping Ratio Estimation

To estimate the 1st and 2nd mode natural frequencies and damping ratios of the model, the values near the frequency peaks (representing the single degree-of-freedom density function of that particular mode) are separated using an ideal band-pass filter as shown in Figure 5b. Since the width of this filter can affect the mode separation, different band-pass filter widths, BPF_n, are tested in the analysis. The BPF_n is selected based on the accuracy of the autocorrelation function, the estimated natural frequency and damping ratio compared

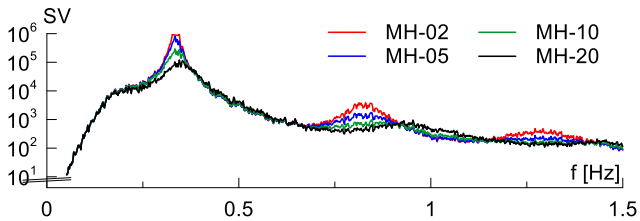

Figure 4. 1st SV distributions of the PSD

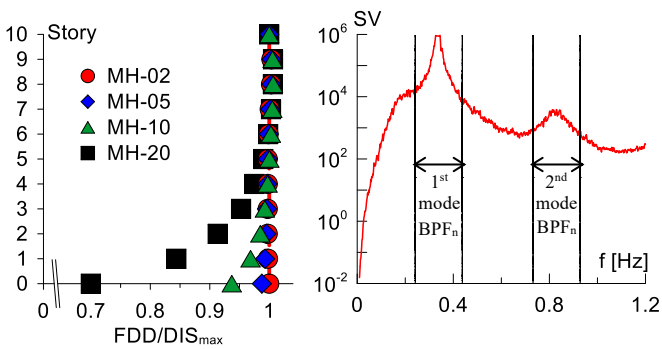

(a) Mode shapes (b) Band-pass filter

Figure 5. Mode shape estimation and mode separation

with theoretical values.

The FDD autocorrelation function is calculated by isolating the SV of each mode and converting it to the time-domain using the inverse Fast Fourier transform. Based on the autocorrelation function comparison in Figure 6, the model with low damping ratio (MH-02) has good agreement with the theoretical autocorrelation function when $BPF_n = 4$. For the model with high damping (MH-20), $BPF_n = 3$ obtained the best results for damping estimation despite the amplitude discrepancies in the estimated autocorrelation function.

Using the autocorrelation function and least squares method, the natural frequency and damping ratio are calculated. The results are shown in Figure 7 and Table 2. Similar to Figure 5a, the results show that the higher the isolation layer damping, the less accurate the estimated parameters (particularly the second mode damping ratio).

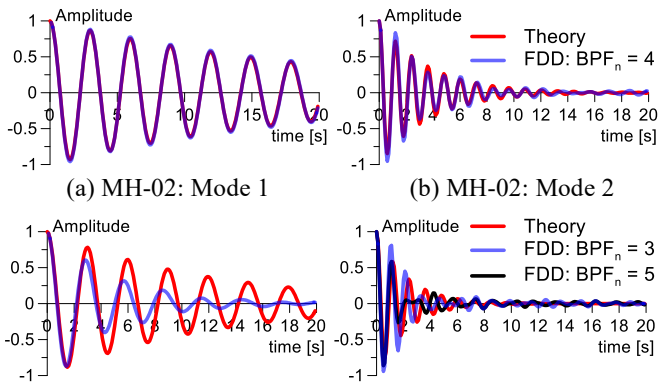

(a) MH-02: Mode 1 (b) MH-02: Mode 2

(c) MH-20: Mode 1 (d) MH-20: Mode 2

Figure 6. Autocorrelation functions

Table 2. FDD results summary

MODEL	FDD Estimates				FDD/Theory (%)			
	$_1\omega$	$_1\omega$	$_1\zeta$	$_2\zeta$	$_1\omega$	$_1\omega$	$_1\zeta$	$_2\zeta$
MH-02	2.10	5.20	0.02	0.05	100	99.9	99.9	97.7
MH-05	2.11	5.20	0.03	0.08	100	99.9	93.3	95.3
MH-10	2.12	5.52	0.06	0.13	99.3	94.4	86.9	89.9
MH-20	2.15	5.10	0.11	0.21	98.9	97.4	88.8	82.7

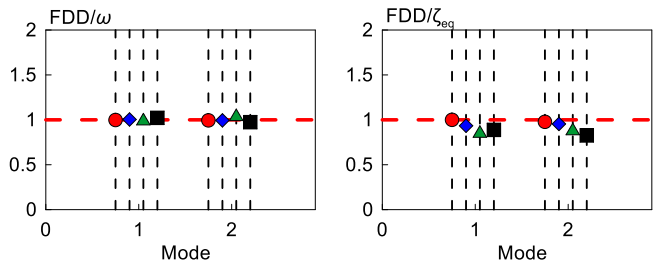

(a) Natural frequency (b) Damping ratio

Figure 7. Accuracy of FDD-estimated parameters

4.4 Wind Force Estimation (using FDD results)

Using the results from FDD, the [K] and [C] matrices are obtained and the wind forces were calculated using Eqs. (7) and (8). The results of the estimated wind forces (Modes 1-11) for the different damping models are shown in Figure 8. The errors in the estimated parameters of the FDD naturally resulted in loss of accuracy in the estimated wind forces. The wind forces estimated in low damping models (MH-02, MH-05, MH-10) were of higher accuracy (generally above 85%) than the high damping models such as MH-20 (average correlation of 71%). Also, for MH-20, the upper stories have

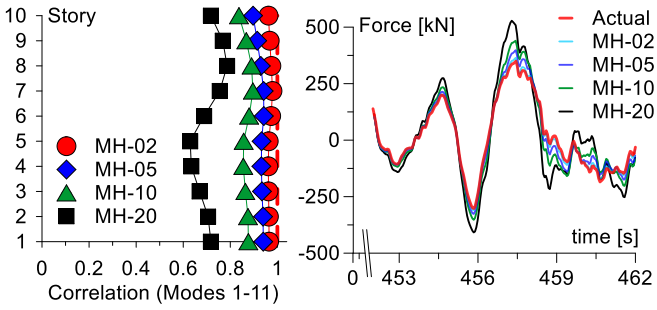

(a) correlation (b) time-history (top story)

Figure 8. Wind force estimation results

better agreement than the lower stories. This behavior is due to the error in the mode shape estimation which shows a similar pattern in Figure 5.

5. Conclusions

This paper investigated the accuracy of modal analysis in identifying the wind forces acting on an elastic base-isolated model whose dynamic parameters are estimated by FDD method. The results show that the wind forces can be estimated with high accuracy (over 85%) for models with an isolator damping of up to 10%.

References

[1] Nakagawa, K., Shimazaki, D., Yoshida, S., & Okada, K. (2015). Seismic Design: Application of Seismic Isolation Systems in Japanese High-Rise Buildings. *CTBUH Journal*, *2*, 36-40

[2] Xue, Huili & Liu, Hongjun & Peng, H.Y. & Luo, Yin & Lin, K.. (2019). Wind Load and Structural Parameters Estimation from Incomplete Measurements. Shock and Vibration. 2019. 1-20. 10.1155/2019/4862983.

[3] Brincker, R., Zhang, L., & Andersen, P. (2000). Output-Only Modal Analysis by Frequency Domain Decomposition. In P. Sas, & D. Moens (Eds.), Proceedings of ISMA25: 2000 International Conference on Noise and Vibration Engineering (pp. 717-723). Katholieke Universiteit, Leuven.

[4] Lee, Jiang & Kelly, James. (2019). The effect of damping in isolation system on the performance of base-isolated system. Journal of Rubber Research. 22. 10.1007/s42464-019-00012-z.

[5] Brincker, R., Ventura, C., & Andersen, P. (2003). Why Output Only Modal Analysis is a Desirable Tool for a Wide Range of Practical Applications. In Proceedings of IMAC-21: A Conference on Structural Dynamics, February 3-6, 2003, The Hyatt Orlando, Kissimmee, Florida (pp. 265-272). Society for Experimental Mechanics.

[6] Kaynia A. M., Veneziano D., Biggs J. (1981) Seismic effectiveness of tuned mass dampers, Journal of the Structural Division ASCE, Vol. 107, No. 9, pp.1465-1484..

*1 東京工業大学 大学院生
*2 東京工業大学 准教授・博士（工学）
*3 東京工業大学 助教・Ph. D.

* Graduate Student, Tokyo Institute of Technology *1
* Associate Professor, FIRST, Tokyo Institute of Technology, Dr. Eng.*2
* Assistant Professor, FIRST, Tokyo Institute of Technology, Ph.D.*3